Volume 1, Number 1

JPCR | JOURNAL OF PEDIATRIC CASE REPORTS

A MULTIDISCIPLINARY JOURNAL OF CASE REPORTS

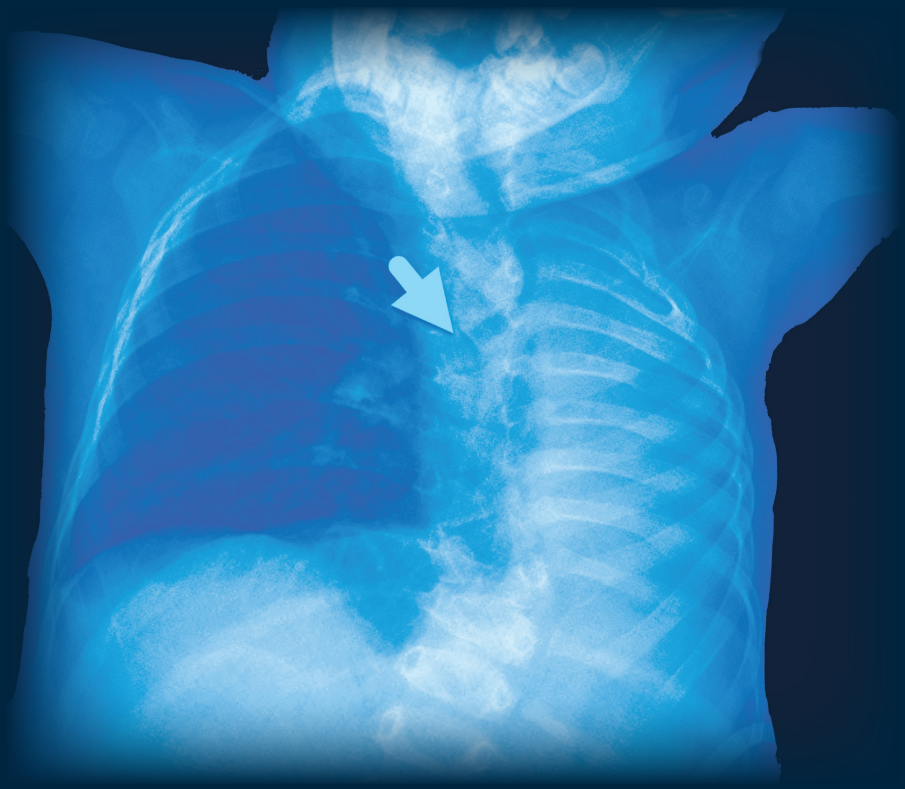

Modified Davis Intubated Ureterotomy

Morgagni Hernia: An Adult with a Congenital Anomaly

Pulmonary Agenesis

Arthrogryposis Multiplex Congenita

Fetal Ureteropelvic Junction Obstruction

Tracheobronchomalacia

www.journalofpediatriccasereports.com

JPCR JOURNAL OF PEDIATRIC CASE REPORTS

A MULTIDISCIPLINARY JOURNAL OF CASE REPORTS

Anderson Publishing, Ltd
180 Glenside Avenue,
Scotch Plains, NJ 07076
Tel: 908-271-8644

VOLUME 1 NUMBER 1

Modified Davis Intubated Ureterotomy

Molly J. Pasque, BS; Richard B. Towbin, MD; Carrie M. Schaefer, MD; Alexander J. Towbin, MD

Abstract

Patients with ureteral injuries who lack enough tissue to perform reanastomosis or a transureteroureterostomy are candidates for a modified Davis ureterotomy. The minimally invasive Davis ureterotomy can effectively bridge large and small ureteral defects.

Keywords: genitourinary tract, ureter, IR procedure

Case Summary

A teenager with a malignant left retroperitoneal paraganglioma, with bone metastases including vertebrae and skull, ultimately underwent surgical resection of the retroperitoneal mass. Then, 6 weeks post resection, on a follow-up US, there had been interval development of left hydronephrosis and a large left retroperitoneal fluid collection, confirmed to be a urinoma on a CT of the abdomen and pelvis. A percutaneous left nephrostomy tube was placed, as well as a percutaneous drainage catheter in the retroperitoneal urinoma. There was an inability to traverse the ureteral defect via a retrograde approach, and a modified percutaneous Davis intubated ureterotomy (DIU) was successfully performed to traverse the ureteral defect from an antegrade and retrograde approach.

Imaging Findings

A multiphase contrast-enhanced CT of the abdomen and pelvis obtained 6 weeks post-left retroperitoneal mass resection demonstrated moderate left hydronephrosis and extravasation of contrast from the proximal left ureter into a large left retroperitoneal urinoma on delayed images (Figure 1A-C). There was no opacification of the distal ureter. A percutaneous left nephrostomy tube was then placed as well as a percutaneous drainage catheter into the urinoma (Figure 2). Subsequently, a percutaneous DIU was performed, with placement of a double-J ureteral stent traversing the ureteral defect, allowing for antegrade flow of urine from the renal pelvis into the bladder and healing of the proximal ureteral defect (Figures 3A-C, 4).

Diagnosis

Laceration/discontinuity of the ureter post resection of a retroperitoneal paraganglioma

Discussion

Historically, the DIU was performed to treat ureteral strictures.[1] In this case, there was injury of the proximal ureter at the time of resection of the retroperitoneal mass, resulting in a urinoma and discontinuity of the proximal ureter with an approximate 3-cm gap. Thus, a historical surgical procedure to treat ureteropelvic junction strictures, the DIU, was modified to create a percutaneous solution. In the literature, there are 2 separate cases of ureteral intubation procedures for the treatment of iatrogenic injury and/or a traumatic injury of the ureter.[2,3] However, this appears to be the first case using a modified percutaneous DIU to treat a segmental ureteral injury at the time of resection of a retroperitoneal malignancy. This discussion will review both the original procedural steps of the DIU and the histopathology of the healing ureter.

The DIU was introduced in 1943.[1] The procedure was used primarily to treat obstructive ureteral strictures, more commonly in patients in whom the ureter was not long enough to resect the stricture and repair the ureteral defect. In the original DIU, surgical exposure of the kidney and ureter was accomplished.[1] An incision was made in the renal pelvis above and through the ureteral stricture below, and a stent was positioned across the stricture and ureteral defect. It was then left in place for 4-6 weeks.[1,2] Once the stent was removed, the healed ureter would ideally have a lumen diameter more comparable to that of a healthy ureter.

Since its introduction, the intubated ureterotomy has been modified

Affiliations: University of Missouri Kansas City, Kansas City, Missouri (Pasque); Phoenix Children's Hospital, Phoenix, Arizona (RB Towbin, Schaefer); Children's Hospital Medical Center, University of Cincinnati College of Medicine, Cincinnati, Ohio (AJ Towbin).

Disclosures: The authors have no conflicts of interest to disclose. None of the authors received outside funding for the production of this original manuscript and no part of this article has been previously published elsewhere.

https://doi.org/10.37549/JPCR-26-0080

Figure 1. Multiphase CT of the abdomen/pelvis demonstrating urinoma (blue arrow) anterior and inferior to the hydronephrotic left kidney in the transverse plane (A) and sagittal plane (B). (C) A delayed image in the sagittal plane demonstrates contrast in the proximal left ureter (green arrow) and in the urinoma (blue arrow).

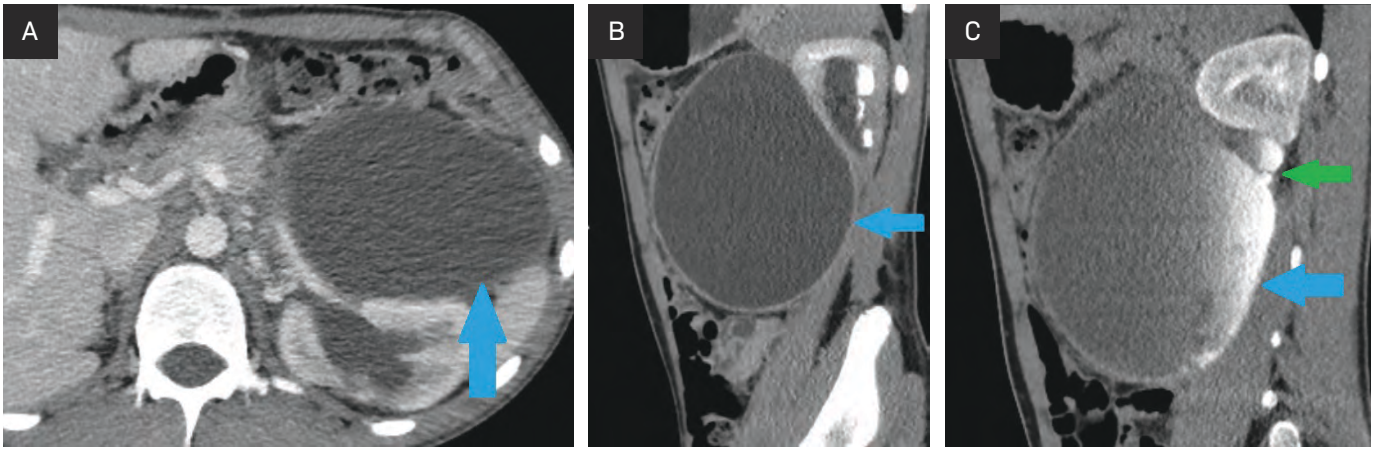

Figure 2. Fluoroscopic save image during contrast injection of the newly placed nephrostomy tube, with extravasation of contrast from the proximal ureter into the urinoma (blue arrow).

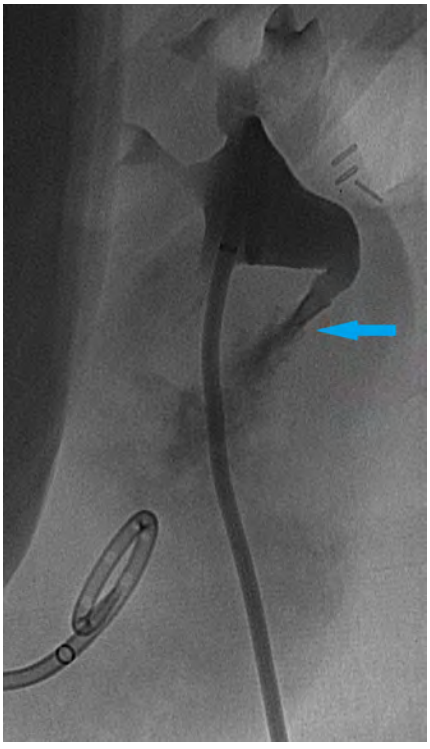

to a percutaneous procedure using a ureteroscope. Hibi describes performing percutaneous intubated ureterotomy procedures by accessing the ureter via a nephrostomy and inserting a ureteroscope. A holmium laser is used to make incisions through the stricture enabling passage of a ureteral stent into the distal normal ureter to be left in place for 6 weeks.[3] Other options for incising the ureter stricture are also utilized, including an Acucise balloon (Applied Medical, Rancho Santa Margarita, California), cold knife, and electrocautery.[3,4] A percutaneous approach decreases the risks of an open procedure, but it can also often be easier for the patient and interventional radiologist and surgeon.[3] This is especially relevant for patients who have strictures secondary to radiation therapy or surrounding fibrosis and adhesions would complicate exposing the ureter in an open surgery.[3] In this case, the DIU procedure was further modified by Towbin and colleagues[5] using invasive, image-guided techniques that can be adapted to treat ureteropelvic junction strictures as well as ureteral injuries ranging from tears to short segment resections.[5] In 2014, Liu and colleagues described an alternative procedure using an endoscope.[6]

In this situation, the ureteral repair was approached antegrade and retrograde, with urology accessing the distal ureter from a retrograde urethral approach. Sheaths and directional catheters over wires were utilized antegrade and retrograde, and the catheters positioned at the junction of the proximal ureter and urinoma from an antegrade approach, and the cephalad aspect of the distal ureteral segment from a retrograde approach, under fluoroscopy. A loop snare was deployed into the urinoma from the retrograde approach, and an angled guidewire advanced into the loop snare from the antegrade approach (Figure 3A,B). Once the wire was snared, the glidewire was withdrawn into and out of the retrograde sheath, thus the wire extended outside of the antegrade and retrograde placed sheaths (a body floss). Subsequently, a double-J ureteral stent was advanced over the wire through the retrograde sheath, through the ureteral defect, and the proximal loop of the stent positioned in the left upper pole calyx, the caudad double-J ureteral stent loop positioned in the urinary bladder (Figure 3C). Additionally, the left nephrostomy tube was replaced.

Thirteen days following double-J ureteral stent placement, contrast injection of the nephrostomy tube demonstrated that contrast traversed the stent lumen with opacification of the urinary bladder, and there was not extravasation of contrast into the urinoma. The nephrostomy tube was removed 15 days following placement of the ureteral stent. A retrograde pyelogram was performed 6 weeks following ureteral stent placement, demonstrating opacification of an intact ureter and nondilated intrarenal

Figure 3. Fluoroscopic save images during percutaneous intubated ureterotomy. (A) The loop snare is open (blue arrow) in the urinoma and placed through the retrograde sheath, with the antegrade wire traversing the open snare (green arrow). (B) The snare is closed around the wire (blue arrow), and the wire is being withdrawn into the retrograde sheath. (C) Double-J ureteral stent traversing the distal and proximal ureter (blue arrow) with the proximal loop in the upper pole calyx (green arrow), which is opacified with contrast.

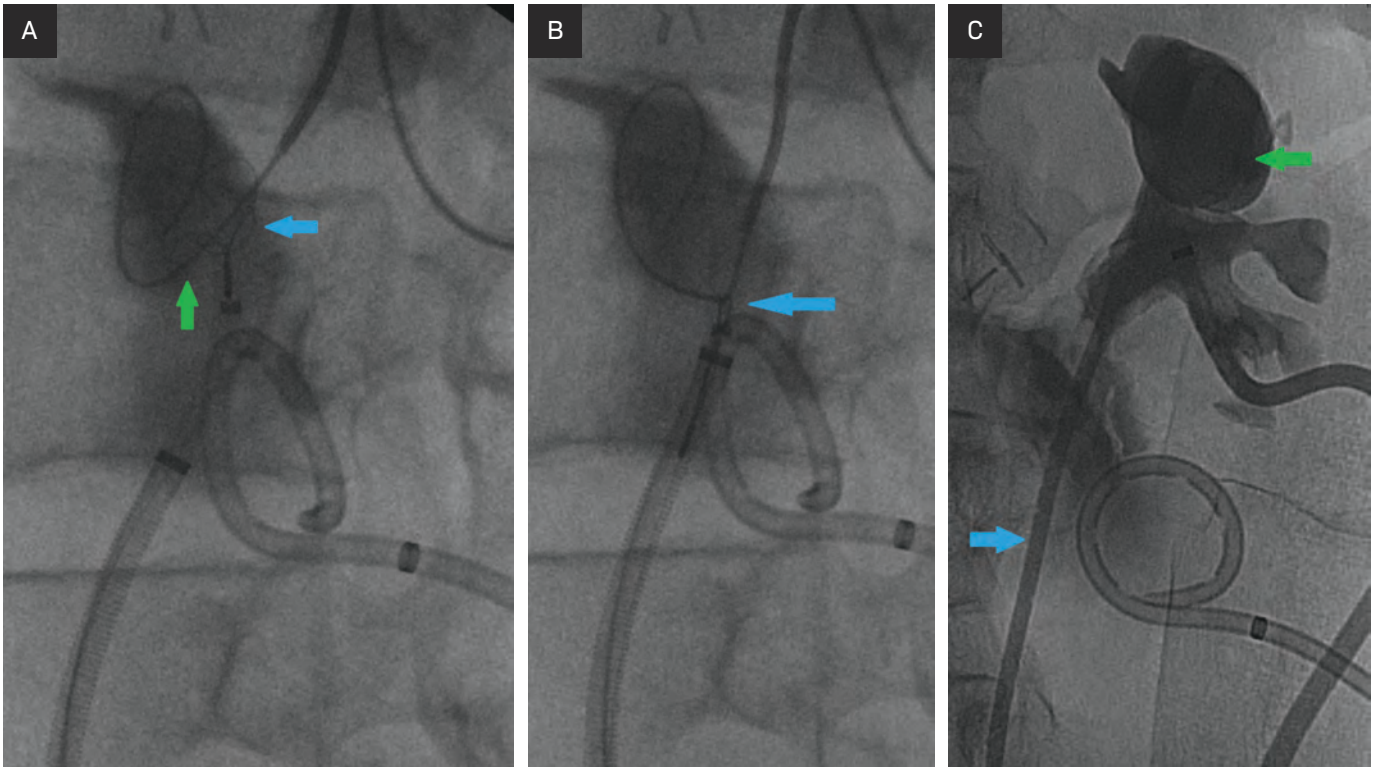

Figure 4. CT 3D rendering of the left double-J ureteral stent (blue arrow), obtained 1 day after placement, with the proximal stent loop in the intrarenal collecting system and the distal loop in the urinary bladder.

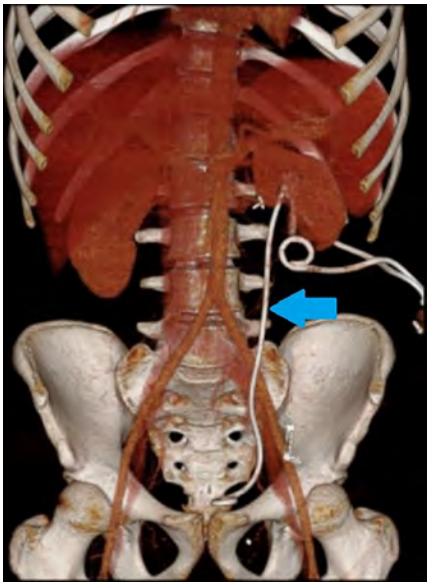

collecting system. A proximal ureteral stricture was identified 2 months following the initial stent placement on a retrograde pyelogram, and interval ureteral stent exchanges were performed out to at least 12 months.

A minimally invasive, image-guided approach for repair of segmental ureteral gaps is an increasingly important topic. Since the introduction of laparoscopic surgery, the rate of ureteral injury has increased, and most injuries are identified postoperatively.[7] The most common urologic structure injured during pelvic surgery is the ureter, with risk factors including obesity, excessive bleeding, enlarged uterus, and adhesions from prior surgeries.[8]

The intubated ureterotomy is successful because of the unique healing process and regeneration capabilities of the ureter. Research into the regeneration process raised the question of whether the smooth muscle can completely regenerate either by muscle cell hypertrophy or true replication.[9] Some studies found that smooth muscle cells did not completely regenerate around the circumference of the ureter; instead, the gap was filled with connective tissue.[2,10] Current research has shown that there is a more complete understanding of how ureteral healing occurs. Uroepithelial regeneration is the initial step in ureter healing, which usually occurs within the first 3 weeks.[11] The stent acts as a guide to direct the epithelial growth so that the gap is closed in an organized manner.[9] Once the epithelium has regenerated, this serves as a foundation for the rest of the ureteral layers to grow. It is believed that stent removal after 3 weeks results in normal healing of the ureter because the epithelium has grown back at that point.[10] Next, the wound begins contracting and the gap is filled with connective tissue.[11,12]

https://doi.org/10.37549/JPCR-26-0080

Lastly, the fibroblasts in the connective tissue are replaced by smooth muscle cells.[12] This regeneration process is the foundation for why intubation and stenting work well in patients with ureteral injuries.

The reported success rate for a DIU approaches 89%.[1] The rate of success using minimally invasive techniques is likely similar; however, no large series are available for guidance. Complications include irregular regeneration, diverticulum formation, and obstruction secondary to strictures or scarring. Other problems that can be identified are infection, urinoma formation, and loss of renal function.

Conclusion

Patients with ureteral injuries who lack enough tissue to perform reanastomosis or a transureteroureterostomy are candidates for a modified Davis ureterotomy. The minimally invasive Davis ureterotomy can effectively bridge large and small ureteral defects.

References

1) Davis DM, Strong GH, Drake WM. Intubated ureterotomy; experimental work and clinical results. *J Urol*. 1948;59(5):851-859. doi:10.1016/S0022-5347(17)69449-7

2) Smart WR. An evaluation of intubation ureterotomy with a description of surgical technique. *J Urol*. 1961;85(4):512-524. doi:10.1016/S0022-5347(17)65372-2

3) Hibi H, Yamada Y, Nonomura H, et al. Percutaneous ureteral incision with a small-caliber flexible ureteroscope. *JSLS*. 2003;7(2):107-110.

4) Arabi M, Mat'hami A, Said MT, et al. Image-guided ureteral reconstruction using rendezvous technique for complex ureteric transection after gunshot injuries. *Avicenna J Med*. 2016;6(1):28-30. doi:10.4103/2231-0770.173581

5) Towbin RB, Wacksman J, Ball WS. Percutaneous pyeloplasty in children: experience in three patients. *Radiology*. 1987;163(2):381-384. doi:10.1148/radiology.163.2.3562817

6) Liu C, Zhang X, Xue D, Liu Y, Wang P. Endoscopic realignment in the management of complete transected ureter. *Int Urol Nephrol*. 2014;46(2):335-340. doi:10.1007/s11255-013-0535-7

7) Pastore AL, Palleschi G, Silvestri L, et al. Endoscopic rendezvous procedure for ureteral iatrogenic detachment: report of a case series with long-term outcomes. *J Endourol*. 2015;29(4):415-420. doi:10.1089/end.2014.0474

8) Lapides J, Caffery EL. Observations on healing of ureteral muscle: relationship to intubated ureterotomy. *J Urol*. 2017;73:47-52. doi:10.1016/S0022-5347(17)67365-8

9) Duque O, Boyarsky S. Ureteral regeneration in dogs: an experimental study bearing on the davis intubated ureterotomy. *J Urol*. 2017;73:53-61. doi:10.1016/S0022-5347(17)67366-X

10) McDonald JH, Calams JA. Experimental ureteral stricture: ureteral regrowth following ureterotomy with and without intubation. *J Urol*. 2017;84:52-59. doi:10.1016/S0022-5347(17)65486-7

11) Trautner K, Raaschou F. Histological examination of the regeneration of urotherthe ureter in dogs after intubated ureterotomy. *J Urol*. 2017;71:274-286. doi:10.1016/S0022-5347(17)67788-7

12) Velardo JT. Histology of the ureter. In: Bergman H, ed. *The ureter*. Springer. 1981. doi:10.1007/978-1-4612-5907-7_2

Morgagni Hernia: An Adult with a Congenital Anomaly

Rachel May, BS; Kevin M. Baskin, MD; Richard B. Towbin, MD; Alexander J. Towbin, MD

Abstract

Although Morgagni hernia is the rarest type of congenital diaphragmatic hernia, it is clinically important due to the potential for delayed diagnosis and associated complications. Its bimodal age distribution underscores the importance of recognizing this condition in both pediatric and adult populations, where symptoms can range from asymptomatic findings to severe pulmonary or gastrointestinal issues. Accurate diagnosis depends on imaging, with lateral chest x-rays often identifying initial signs, while advanced modalities like CT or MRI may provide definitive confirmation.

Keywords: gastrointestinal, stomach, adult with a congenital anomaly

Case Summary

A 40-year-old woman presented with shortness of breath and chest pain.

Imaging Findings

In retrospect, a chest radiograph at initial presentation (Figure 1) and subsequent chest CT (Figure 2) showed a small anterior diaphragmatic hernia containing only omental fat. She continued to experience recurrent chest pain, shortness of breath, and abdominal symptoms without a definitive diagnosis. Comorbidities in this patient included severe degenerative disk disease, asthma, and partially reversible anteroseptal cardiac ischemia. Nine years later, a chest radiograph obtained for difficulty breathing and chest pain demonstrated an enlarged anterior diaphragmatic hernia misdiagnosed as a hiatal hernia at the time. Six months later, she reported worsening chest and back pain, nausea, vomiting, and diarrhea. Retrospective review of an abdominal US from this period showed herniating omental fat in the anterior thorax that was not recognized. Ten years from her initial presentation, after a 60-pound weight loss and recurring symptoms, the patient was admitted to the hospital. A chest x-ray confirmed an enlarging Morgagni hernia (Figure 3). Abdominopelvic CT on the same date (Figure 4) demonstrated the anterior Morgagni hernia and posteriorly a large paraesophageal hernia. Concurrent chest CT imaging (Figure 5) showed the intrathoracic extent of the hernias.

Figure 1. (A) A posteroanterior chest radiograph demonstrating very subtle fat-attenuation tissue herniating into the mediastinum just to the right of midline (arrows). (B) The lateral view shows the same tissue (arrows) in the anterior mediastinum.

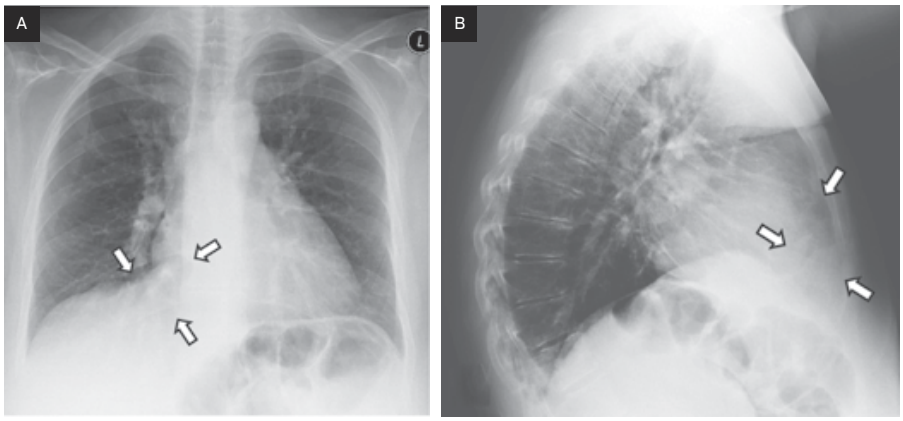

Diagnosis

Morgagni hernia.

Differential diagnosis includes hiatal hernia, cardiophrenic fat pad, pericardial cyst, diaphragmatic eventration,

Affiliations: Lewis University, Romeoville, Illinois (May); Department of Radiology, Conemaugh Memorial Medical Center, Johnstown, Pennsylvania (Baskin); Department of Radiology, Phoenix Children's Hospital, Phoenix, Arizona (RB Towbin); Department of Radiology, Cincinnati Children's Hospital, University of Cincinnati College of Medicine, Cincinnati, Ohio (AJ Towbin).

Disclosures: The authors have no conflicts of interest to disclose. None of the authors received outside funding for the production of this original manuscript and no part of this article has been previously published elsewhere.

https://doi.org/10.37549/JPCR-26-0081

Figure 2. (A) An axial CT section through the lower chest, obtained 3 years after Figure 1, demonstrating omental fat (asterisk) that has herniated into the anterior mediastinum. (B) A mid-sagittal section from the same study showing the omental fat herniating through the anterior defect in the diaphragm (arrowheads) that defines a Morgagni hernia.

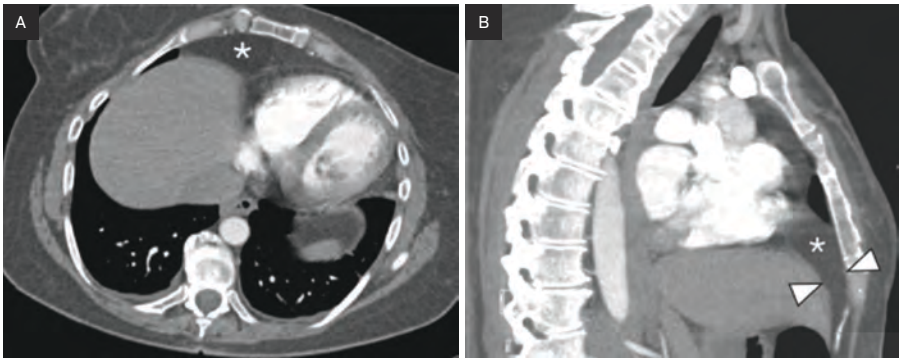

Figure 3. Posteroanterior (A) and lateral (B) chest radiographs obtained 10 years after Figure 1 showing the significant interval increase in the size of the Morgagni hernia (arrows), now containing transverse colon and loops of small bowel in addition to omental fat.

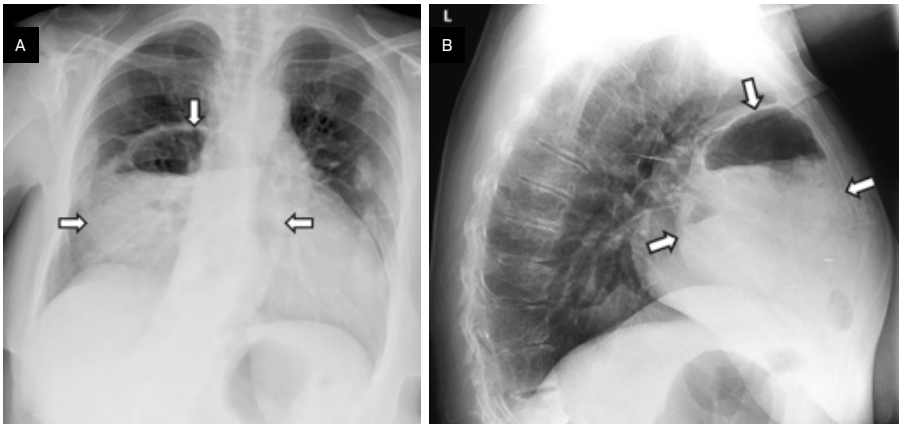

Figure 4. Axial (A) and mid-sagittal (B) abdominopelvic CT sections obtained 10 years after Figure 1 showing the significant interval increase in size of the Morgagni hernia (outlined by arrowheads), located in the right anterior mediastinum, through the expanding sub-costosternal diaphragmatic defect. Note is made of a coexisting paraesophageal hernia (star), with approximately 40% of the stomach within the thoracic cavity.

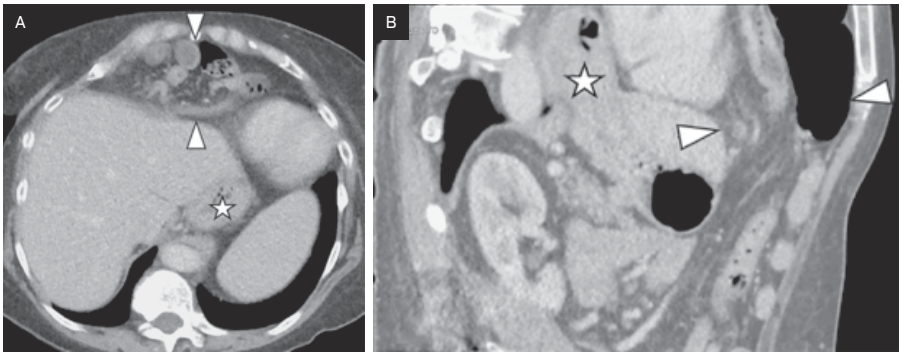

loculated pneumothorax, lower lobe lung collapse or consolidation, lymphoma, or thymic tumor.

Discussion

A Morgagni hernia is the rarest subtype of congenital diaphragmatic hernia (CDH), representing 2-4% of all cases.[1] It results from an anteromedial sub-costosternal diaphragmatic defect defined by the failure of the pars tendinalis of the costochondral arches to fuse with the pars sternalis during embryonic development. Morgagni hernia exhibits a bimodal age distribution, typically presenting in infants and young children, predominantly males, within the first year of life. The estimated incidence is between 1 in 2000 and 1 in 5000 live births. In children, it is often asymptomatic but may present with nonspecific findings such as respiratory distress, failure to thrive, recurrent pulmonary infections, poor feeding, or choking during feeding. In pediatric patients, it is often associated with other congenital abnormalities such as cardiac anomalies and Trisomy 21.[1] In general, those presenting after 8 weeks of life in the pediatric population have a benign course and respond well to surgical repair.[2] In rare cases, Morgagni hernia may present in adulthood, with a mean age at diagnosis of 57 years and a higher prevalence observed in females.[3] Presentation in adults is often (72%) symptomatic, most commonly with pulmonary symptoms.[4] Acute complications, such as intestinal ischemia due to bowel strangulation or gastric volvulus, may also occur.[5]

These hernias are most frequently located on the right side and are characterized by the herniation of abdominal contents into the thoracic cavity.[4] While they most commonly contain omental fat, herniation of the transverse colon, small bowel, stomach, or liver can also occur. Differential considerations on plain chest x-ray include

Figure 5. Axial (A) and mid-sagittal (B) chest CT sections obtained 1 month after Figure 4 demonstrating the intrathoracic extent of the Morgagni hernia (arrowheads) containing loops of colon and small bowel and extending through the developmental defect (black arrows) between the pars tendinalis and the pars sternalis of the diaphragm.

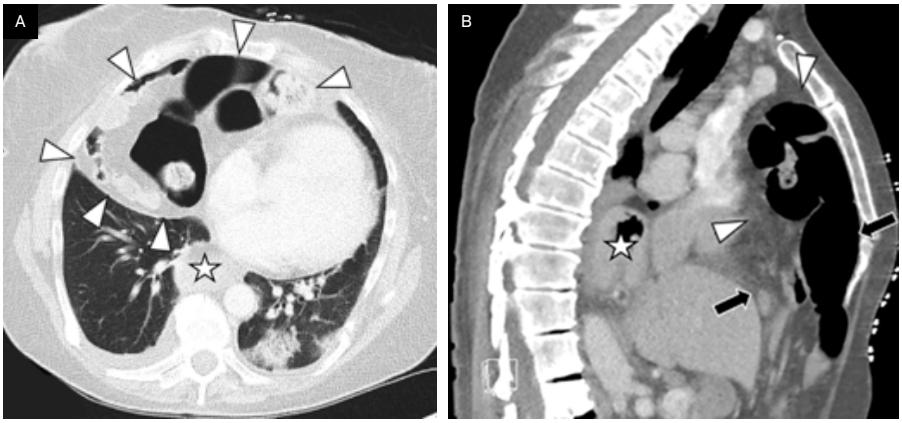

cardiophrenic fat pad, diaphragmatic eventration, pericardial cyst, loculated pneumothorax, lower lobe lung collapse or consolidation, lymphoma, or thymic tumor. Diagnosis is often made incidentally on lateral chest x-ray, especially when bowel is visible anteriorly within the thoracic cavity.[1] If suspected, the diagnosis may be confirmed when abdominal CT or MRI demonstrates intrathoracic herniation of omental fat or air-filled viscera anteriorly,[6] with loss of continuity between the diaphragm and the lower sternum, especially on a sagittal view. A barium study or US may support the diagnosis.[7]

Conclusion

Although Morgagni hernia is the rarest type of CDH, it is clinically important due to the potential for delayed diagnosis and associated complications. Its bimodal age distribution underscores the importance of recognizing this condition in both pediatric and adult populations, where symptoms can range from asymptomatic findings to severe pulmonary or gastrointestinal issues. Accurate diagnosis depends on imaging, with lateral chest x-rays often identifying initial signs, while advanced modalities like CT or MRI may provide definitive confirmation.

References

1) Svetanoff WJ, Sharma S, Rentea RM. Morgagni hernia. In: *StatPearls* [Internet]. StatPearls Publishing. 2025.

2) Berman L, Stringer D, Ein SH, Shandling B. The late-presenting pediatric morgagni hernia: a benign condition. *J Pediatr Surg*. 1989;24(10):970-972. doi:10.1016/s0022-3468(89)80193-9

3) Archer JP, Williams N. Non-operative management of a large morgagni hernia-an alternative approach?. *J Surg Case Rep*. 2023;2023(1):rjac614. doi:10.1093/jscr/rjac614

4) Horton JD, Hofmann LJ, Hetz SP. Presentation and management of morgagni hernias in adults: a review of 298 cases. *Surg Endosc*. 2008;22(6):1413-1420. doi:10.1007/s00464-008-9754-x

5) Sonthalia N, Ray S, Khanra D, et al. Gastric volvulus through morgagni hernia: an easily overlooked emergency. *J Emerg Med*. 2013;44(6):1092-1096. doi:10.1016/j.jemermed.2012.11.103

6) Kuikel S, Shrestha S, Thapa S, et al. Morgagni hernia in adult: a case report. *Int J Surg Case Rep*. 2021;85:106286. doi:10.1016/j.ijscr.2021.106286

7) Shi H-Q, Chen W-J, Yin Q, Zhang X-H. Ultrasound diagnosis of congenital morgagni hernias: ten years of experience at two chinese centers. *World J Clin Cases*. 2024;12(3):495-502. doi:10.12998/wjcc.v12.i3.495

https://doi.org/10.37549/JPCR-26-0081

Pulmonary Agenesis

Vincent F. Carfagno, BS; Richard B. Towbin, MD; Carrie M. Schaefer, MD; Alexander J. Towbin, MD

Abstract

Pulmonary agenesis is a rare developmental malformation that presents with nonspecific respiratory symptoms, a small hemithorax, and unilateral absence of breath sounds. Diagnosis is based on clinical suspicion and imaging findings. Radiological workup is essential for diagnosis and helps to distinguish pulmonary agenesis from other developmental malformations, such as pulmonary atresia and aplasia, and acquired conditions, such as foreign bodies and pneumonia.

Keywords: thorax, airway, congenital

Case Summary

A twin female toddler born at 32 weeks of gestation presented with tachypnea on exertion. The toddler's medical history includes a vascular ring, gastrostomy tube dependence, and agenesis of the left lung and pulmonary veins.

Imaging Findings

Chest radiograph (Figure 1) demonstrated a hyperinflated right lung with a mediastinal shift toward an opaque and small left hemithorax. There was no visible aeration of the left tracheobronchial tree. Contrast-enhanced CT (CECT) (Figure 2) displayed leftward mediastinal shift, with the absence of the left lung and pulmonary vasculature. Bronchoscopy confirmed absence of the left mainstem bronchus.

Diagnosis

Pulmonary agenesis.

The differential diagnosis for tachypnea on exertion includes respiratory pathology such as bronchopulmonary dysplasia, asthma, and pneumonia. Nonrespiratory causes include developmental heart defects and metabolic disturbance. The differential diagnosis for radiographic imaging demonstrating an opaque hemithorax with contralateral lung hyperinflation includes pulmonary agenesis, pulmonary aplasia, atelectasis, and pneumonectomy.

Discussion

Pulmonary agenesis (PA) is a developmental malformation with absence of one or both lungs, bronchi, pulmonary parenchyma, and vasculature.[1] This developmental anomaly should not be confused with pulmonary atresia, a heart valve defect resulting in an absent pulmonary valve. While bilateral pulmonary agenesis may occur, it is not compatible with life. Patients with unilateral agenesis have a variable prognosis, with 50% dying within the first 5 years of life and others having a normal lifespan with minimal symptoms.[2-5] Mortality rates in patients with unilateral pulmonary agenesis vary based on the presence of recurrent infections, associated malformations, and the side of agenesis. Right-sided pulmonary agenesis has a higher risk of mortality due to more pronounced mediastinal shift and resultant tracheal compression.[2]

Pulmonary agenesis is rare, occurring in 1 in 10,000-15,000 births.[3] Unilateral pulmonary agenesis occurs on the right and left sides with equal frequency. It may occur in isolation or as part of a group of related developmental malformations, with the latter portending a worse prognosis.[6] If not diagnosed in utero,

Figure 1. Chest radiograph showing a hyperinflated right lung. The left hemithorax is small, and there is a complete leftward mediastinal shift. The right mainstem bronchus (arrow) is visible. There is no visible left mainstem bronchus.

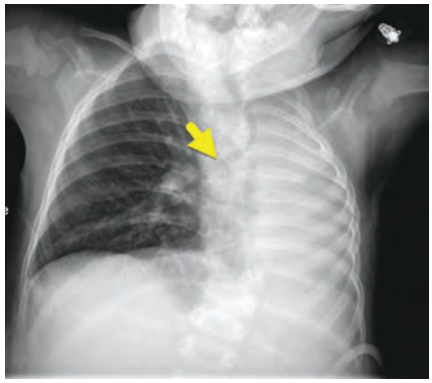

Affiliations: Midwestern University Arizona College of Osteopathic Medicine, Glendale Arizona, Glendale, Arizona (Carfagno); Department of Radiology, Phoenix Children's Hospital, Phoenix, Arizona (RB Towbin, Schaefer); Department of Radiology, Cincinnati Children's Hospital, University of Cincinnati College of Medicine, Cincinnati, Ohio (AJ Towbin).
Disclosures: The authors have no conflicts of interest to disclose. None of the authors received outside funding for the production of this original manuscript and no part of this article has been previously published elsewhere.

https://doi.org/10.37549/JPCR-26-0079

Figure 2. (A) Axial contrast-enhanced CT of the chest in lung windows showing a hyperinflated right lung and absence of the left lung. There is a leftward shift of the heart and mediastinum. (B) Axial contrast-enhanced CT of the chest in soft tissue windows showing the right pulmonary artery (arrow) and absence of the left pulmonary artery. (C) Coronal minimum intensity projection image and (D) 3D-reformatted image of the airway highlighting the trachea and right mainstem bronchus. The right lower lobe bronchus (arrow) arises from the mainstem bronchus. There is no left mainstem bronchus.

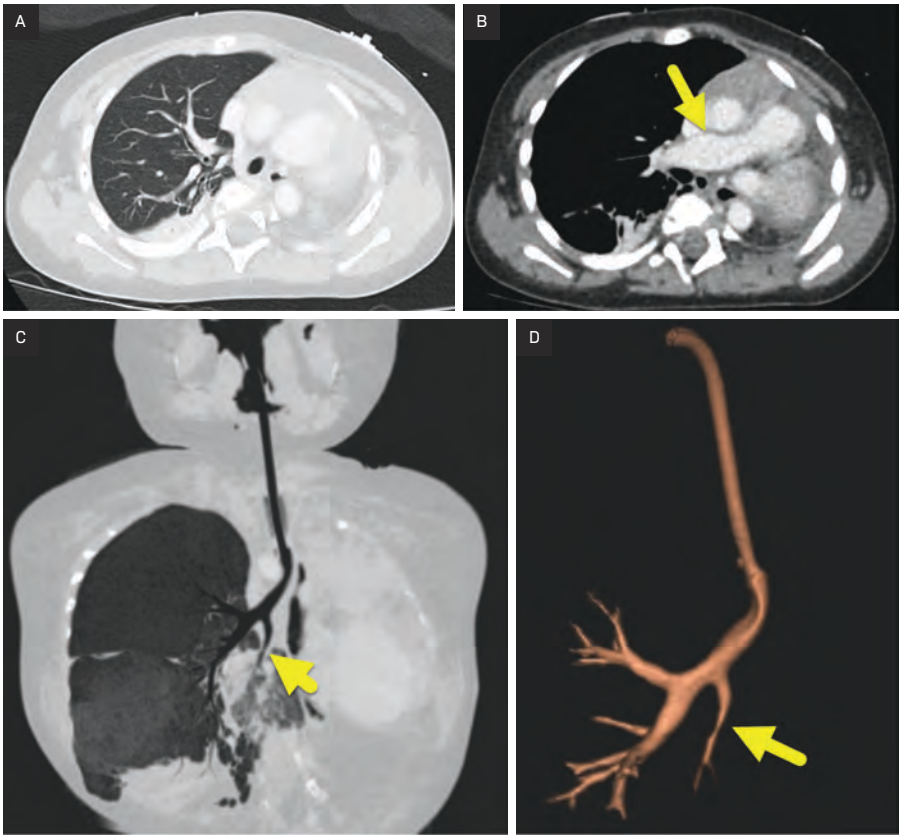

patients may present with nonspecific symptoms. An ultimate diagnosis is made with chest imaging. Radiological workup begins with a chest radiograph, which shows a hyperinflated contralateral lung and a small hemithorax with ipsilateral mediastinal shift.[4] Transthoracic echocardiogram with Doppler may also be utilized to evaluate for agenesis of pulmonary vasculature on the affected side.

Diagnosis is confirmed with CECT displaying a single mainstem bronchus, unilateral absence of lung parenchyma, compensatory hyperinflated contralateral lung, and a single-branch pulmonary artery. CT can also highlight tracheobronchial branching abnormality.[4] Intravenous contrast can demonstrate associated vascular abnormalities such as pulmonary artery hypoplasia, right aortic arch, anomalous venous return, septal defects, and Tetralogy of Fallot.

Of note, CECT may also help distinguish unilateral pulmonary agenesis from the similar, yet distinct unilateral pulmonary aplasia. While both malformations involve the absence of pulmonary parenchyma and vasculature, pulmonary aplasia maintains 2 mainstem bronchi, one of which ends in a blind-ended pouch. This is due to developmental arrest occurring at a later stage in fetal lung development after the formation of the mainstem bronchi.

Although bronchoscopy is not necessary for confirming the diagnosis of pulmonary agenesis, it may be used instead of imaging if the differential diagnosis includes other causes of unilateral absence of breath sounds.[7, 8] If bronchoscopy is performed, the absence of a mainstem bronchus on the affected side confirms the diagnosis of unilateral pulmonary agenesis.

Respiratory insufficiency may occur in patients with unilateral pulmonary agenesis due to recurrent respiratory infections, tracheal compression, and pulmonary hypertension.[2,4] Because infection is a significant source of morbidity, patients may be treated with prophylactic antibiotics. Additionally, because mediastinal shift may lead to tracheal kinking and compression, tracheal stenting or tracheoplasty may be performed to improve aeration of the lung.[9]

The outcome of children with PA is variable and is associated with associated anomalies and the degree of respiratory failure. In general, over 50% of infants die by age 5 years, with about a third passing in the first year. In contrast, children with no associated malformations often live into adulthood.

Conclusion

Pulmonary agenesis is a rare developmental malformation that presents with nonspecific respiratory symptoms, a small hemithorax, and unilateral absence of breath sounds. Diagnosis is based on clinical suspicion and imaging findings. Radiological workup is essential for diagnosis and helps to distinguish pulmonary agenesis from other developmental malformations, such as pulmonary atresia and aplasia, and acquired conditions, such as foreign bodies and pneumonia.

References

1) Fukuoka S, Yamamura K, Nagata H, et al. Clinical outcomes of pulmonary agenesis: a systematic review of the literature. *Pediatr Pulmonol.* 2022;57(12):3060-3068. doi:10.1002/ppul.26135

2) Jentzsch NS. Unilateral pulmonary agenesis. *J Bras Pneumol.* 2014;40(3):322-324. doi:10.1590/s1806-37132014000300017

3) Kumar B, Kandpal DK, Sharma C, Sinha DD. Right lung agenesis. *Afr J Paediatr Surg*. 2008;5(2):102-104. doi:10.4103/0189-6725.44189

4) Chassagnon G, Morel B, Carpentier E, Ducou Le Pointe H, Sirinelli D. Tracheobronchial branching abnormalities: lobe-based classification scheme. *Radiographics*. 2016;36(2):358-373. doi:10.1148/rg.2016150115

5) Dinamarco PVV, Ponce CC. Pulmonary agenesis and respiratory failure in childhood. *Autops Case Rep*. 2015;5(1):29-32. doi:10.4322/acr.2014.046

6) Malcon MC, Malcon CM, Cavada MN, Caruso PEM, Real LF. Unilateral pulmonary agenesis. *J Bras Pneumol*. 2012;38(4):526-529. doi:10.1590/s1806-37132012000400016

7) Alwan A,Y, Mohammoud S M, Assefa AZ Y, N, S. Incidental pulmonary agenesis with multiple associated anomalies: A case report.. *Radiol Case Rep.*. 2023;18(10):3724-3728. doi: 10.1016/j.radcr.2023.08.002.

8) Shrikhande DY, Singh G, Kunal A, Niranjan BK, Kumar CA. Unilateral pulmonary agenesis-a rare cause of respiratory distress in infancy. *Med J Armed Forces India*. 2012;68(2):176-178. doi:10.1016/S0377-1237(12)60026-4

9) Khurram MSA, Rao SP, Vamshipriya A. Pulmonary agenesis: a case report with review of literature. *Qatar Med J*. 2013;2013(2):38-40. doi:10.5339/qmj.2013.14

Arthrogryposis Multiplex Congenita

Travis A. Seideman, BS; Richard B. Towbin, MD; Carrie M. Schaefer, MD; Alexander J. Towbin, MD

Abstract

Arthrogryposis multiplex congenita (AMC) is a multietiologic congenital syndrome resulting from decreased fetal movement and defined by joint contractures involving 2 or more body regions. The 6 major etiologic categories include neuropathic abnormalities, muscle abnormalities, connective tissue abnormalities, uterine space limitations, intrauterine vascular compromise, and maternal disease. Prenatal US most commonly detects joint contractures during the second or third trimester, although first-trimester findings such as increased nuchal translucency or congenital anomalies may suggest the diagnosis earlier. In cases where fetal movement is not assessed, diagnosis may be delayed until birth. Careful attention to imaging findings is essential when evaluating any pregnancy in which decreased fetal movement is reported or AMC is suspected.

Keywords: musculoskeletal, syndrome, congenital

Clinical Summary

A G5P2 woman presented for level 2 US at 25 weeks of gestation after club foot was identified on level 1 US.

Imaging Findings

Fetal US (Figure 1) and MRI (Figure 2) showed fixed extension of the elbows and flexion of the wrists. Bilateral clubfoot was also present.

Diagnosis

Arthrogryposis multiplex congenita (AMC) is an umbrella term encompassing a wide range of congenital conditions characterized by multiple joint contractures.

The differential diagnosis is broad and includes distal arthrogryposis, congenital bony fusions, contractural arachnodactyly, multiple pterygium syndrome, and other disorders that affect both the limbs and additional organ systems.

Discussion

AMC is a congenital syndrome defined as a group of conditions characterized by joint contractures involving 2 or more body regions.[1] The unifying mechanism across all forms of AMC is decreased fetal movement (fetal akinesia).[2] When movement is restricted early in gestation, the resulting contractures are typically more severe.[3] The causes of fetal akinesia are diverse and often multifactorial. However, they can generally be grouped into 6 major categories: neuropathic abnormalities, muscle abnormalities, connective tissue abnormalities, uterine space limitations, intrauterine vascular compromise, and maternal disease.[2]

The 6 etiologic categories of AMC encompass a wide range of underlying abnormalities. Neuropathic causes involve both the central and peripheral nervous systems and include cerebellar hypoplasia, spinal muscular atrophy (SMA), and other anterior horn cell diseases.[2,4] Muscle-related causes include maternal antibody translocation in myasthenia gravis, congenital muscular dystrophies, and mitochondrial disorders.[2,4] Connective tissue abnormalities may result from normal tissue forming at inappropriate attachment sites or from intrinsic connective tissue defects such as dystrophic dysplasia.[2] Space limitations within the uterus, as seen with oligohydramnios, fibroids, uterine growths, or multiple gestations, can also contribute to the development of AMC.[2,4] Intrauterine vascular compromise leads to decreased blood flow, which can damage fetal nerves and muscles and result in akinesia.[2] Maternal factors, including infections, trauma, and exposure to teratogenic medications, have also been implicated.[2,5,6] Notably, many chromosomal deletion and duplication syndromes have been associated with AMC,[5] and more than 400 specific conditions and over 400 genes have been linked to its development.[5,7]

Individuals with AMC have restricted joint motion that may be accompanied by varying degrees of muscle weakness. These musculoskeletal abnormalities result from reduced fetal movement,

Affiliations: University of Arizona College of Medicine, Phoenix, Arizona (Seideman); Department of Radiology, Phoenix Children's Hospital, Phoenix, Arizona (RB Towbin, Schaefer); Department of Radiology, Cincinnati Children's Hospital, University of Cincinnati College of Medicine, Cincinnati, Ohio (AJ Towbin).
Disclosures: The authors have no conflicts of interest to disclose. None of the authors received outside funding for the production of this original manuscript and no part of this article has been previously published elsewhere.

https://doi.org/10.37549/JPCR-26-0078

Figure 1. Fetal US performed at 25 weeks of gestational age showing (A) fixed extension of the elbow (arrowhead) and flexion of the wrist (arrow). (B) Imaging of the left lower extremity showing a clubfoot (arrow).

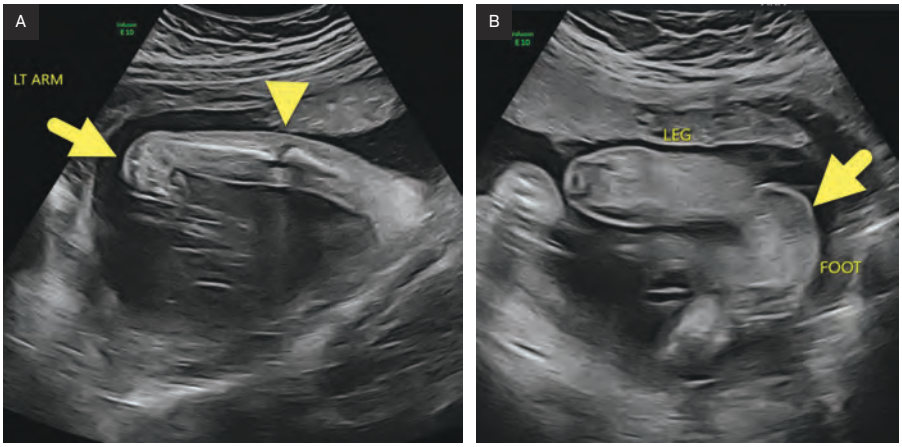

Figure 2. Fetal MRI performed at 25 weeks of gestational age showing (A) fixed extension of the elbow (arrowhead) and flexion of the wrist (arrow). (B) Imaging of the left lower extremity showing a club foot (arrow).

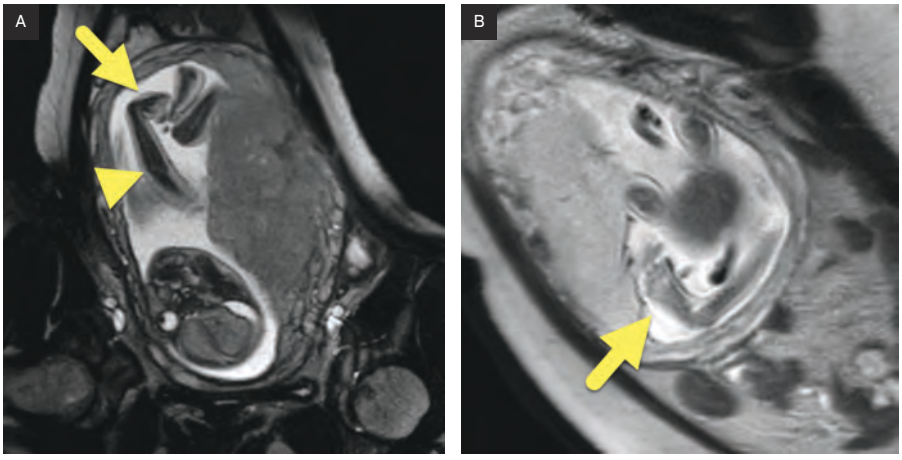

which leads to fixed joint positions and muscle imbalance. In addition to limb contractures, spinal deformities such as scoliosis or kyphosis may be present at birth or develop later in childhood or adolescence. Other organ systems, including the central nervous system (CNS), respiratory, gastrointestinal, and genitourinary systems, may also be affected. Cognitive impairment can occur when the CNS is involved, but sensation is typically preserved. The overall impact on function depends on the degree of musculoskeletal and systemic involvement, with outcomes ranging from mild limitations in mobility to severe lifelong disability.[1]

The clinical presentation of AMC is highly variable, reflecting the diversity of underlying causes. The most common subtype, amyoplasia, accounts for approximately one-third of cases and represents the classic form of AMC. Amyoplasia is characterized by underdevelopment of skeletal muscle and replacement of muscle tissue with fibrofatty tissue. Affected patients typically demonstrate symmetric flexion of the wrists, extension of the elbows, internal rotation of the shoulders, and severe lower-extremity contractures. Additional findings may include decreased muscle bulk, body weight below the 10th percentile, shortened limbs, and dimpling over affected joints. Other presentations may involve only the limbs, primarily the distal limbs, or combinations of limb and systemic involvement, including neuromuscular disorders with associated cognitive or nervous system abnormalities.[5]

US is the primary tool for prenatal diagnosis of AMC.[5] Findings are most often detected in the second or third trimester, typically following maternal reports of reduced fetal movement. At this stage, US can readily identify most types of arthrogryposes. The most common contracture observed is clubfoot, although additional findings may include internal rotation or adduction of the shoulders, abnormal flexion or extension of the elbows, ulnar deviation of the wrists, hip dislocation, and clenched hands.[8] Earlier diagnosis is also possible, as fetal movement can be visualized by US as early as 8 weeks of gestation.[8] In the first trimester, secondary findings such as increased nuchal translucency, cystic hygroma, or a hypoplastic mandible should prompt further evaluation.

In the late second and third trimesters, fetal MRI complements US by identifying potential CNS causes of AMC, including cortical atrophy, lissencephaly, spinal cord atrophy, and cerebellar or pontine hypoplasia.[9] Additional prenatal MRI findings may include hypoplastic lungs, muscular atrophy, growth restriction, craniofacial abnormalities, scoliosis, a short umbilical cord, and abnormal amniotic fluid volume.[8] After birth, radiographs can help identify joint dislocations, ankylosis, bony disproportion, scoliosis, or fusions. Postnatal MRI and US can further evaluate the CNS and musculature to characterize the extent and underlying cause of abnormalities.[5]

The prognosis of AMC varies widely and depends on the underlying etiology and

the severity of contractures. Progressive neuromuscular disorders such as SMA are associated with poorer outcomes compared with contractures resulting from reversible mechanical factors such as oligohydramnios. Children with mild contractures may achieve normal development after appropriate treatment, whereas those with severe, fixed deformities often require lifelong therapy and may experience limited functional independence.[2]

Conclusion

AMC is a multietiologic congenital syndrome resulting from decreased fetal movement and defined by joint contractures involving 2 or more body regions. The 6 major etiologic categories include neuropathic abnormalities, muscle abnormalities, connective tissue abnormalities, uterine space limitations, intrauterine vascular compromise, and maternal disease. Prenatal US most commonly detects joint contractures during the second or third trimester, although first-trimester findings such as increased nuchal translucency or congenital anomalies may suggest the diagnosis earlier. In cases where fetal movement is not assessed, diagnosis may be delayed until birth. Careful attention to imaging findings is essential when evaluating any pregnancy in which decreased fetal movement is reported or AMC is suspected.

References

1) Dahan-Oliel N, Cachecho S, Barnes D, et al. International multidisciplinary collaboration toward an annotated definition of arthrogryposis multiplex congenita. *Am J Med Genet C Semin Med Genet*. 2019;181(3):288-299. doi:10.1002/ajmg.c.31721

2) Kiefer J, Hall JG. Gene ontology analysis of arthrogryposis (multiple congenital contractures). *Am J Med Genet C Semin Med Genet*. 2019;181(3):310-326. doi:10.1002/ajmg.c.31733

3) Hall JG. Arthrogryposis multiplex congenita: etiology, genetics, classification, diagnostic approach, and general aspects. *J Pediatr Orthop B*. 1997;6(3):159-166.

4) Moessinger AC. Fetal akinesia deformation sequence: an animal model. *Pediatrics*. 1983;72(6):857-863.

5) Gordon N. Arthrogryposis multiplex congenita. *Brain Dev*. 1998;20(7):507-511. doi:10.1016/s0387-7604(98)00037-0

6) Hall JG. Arthrogryposis (multiple congenital contractures): diagnostic approach to etiology, classification, genetics, and general principles. *Eur J Med Genet*. 2014;57(8):464-472. doi:10.1016/j.ejmg.2014.03.008

7) van der Linden V, Filho ELR, Lins OG, et al. Congenital zika syndrome with arthrogryposis: retrospective case series study. *BMJ*. 2016;354:i3899. doi:10.1136/bmj.i3899

8) Skaria P, Dahl A, Ahmed A. Arthrogryposis multiplex congenita in utero: radiologic and pathologic findings. *J Matern Fetal Neonatal Med*. 2019;32(3):502-511. doi:10.1080/14767058.2017.1381683

9) Fedrizzi E, Botteon G, Inverno M, et al. Neurogenic arthrogryposis multiplex congenita: clinical and MRI findings. *Pediatr Neurol*. 1993;9(5):343-348. doi:10.1016/0887-8994(93)90102-i

https://doi.org/10.37549/JPCR-26-0078

Fetal Ureteropelvic Junction Obstruction

Tal A. Chamdi, BS; Richard B. Towbin, MD; Carrie M. Schaefer, MD; Alexander J. Towbin, MD

Abstract

Ureteropelvic junction obstruction is the most common cause of congenital hydronephrosis and typically presents with dilation of the renal pelvis and calyces without associated ureteral dilation. Although many cases are suspected prenatally as urinary tract dilation, definitive evaluation occurs postnatally through integration of US findings and functional assessment. US remains the primary imaging modality, with CT or MR urography used when additional anatomic detail is required, particularly to evaluate for extrinsic causes. Renal drainage and differential function are most assessed with mercaptoacetyltriglycine-3 diuretic renography. Management is individualized based on symptoms, severity of dilation, and renal function. While many children are managed conservatively, surgical pyeloplasty is indicated in patients with significant obstruction or declining function and is associated with favorable long-term outcomes.

Keywords: genitourinary, renal, obstruction

Case Summary

A pregnant woman presented at 35 weeks' gestation for advanced imaging following detection of prenatal hydronephrosis on routine screening US.

Imaging Findings

Prenatal US (Figure 1) and MRI (Figure 2) confirmed marked pelvocaliectasis of the right kidney. The right ureter was not visible. Postnatal US (Figure 3) showed similar findings. Tc-99m mercaptoacetyltriglycine (MAG) nuclear medicine study (Figure 4) confirms severe delay in the excretion of the radiopharmaceutical from the right kidney. Intraoperative ureteroscopy with contrast injection confirmed a right ureteropelvic junction (UPJ) obstruction (Figure 5).

Diagnosis

Fetal UPJ obstruction.

The differential diagnosis of isolated pelvocaliectasis includes intrinsic UPJ obstruction, extrarenal pelvis, parapelvic cyst, and vesicoureteral reflux.

Discussion

UPJ obstruction is the most common cause of congenital hydronephrosis and the most frequent obstructive uropathy in children. It occurs in approximately 1 in 1000 newborns, demonstrates a male predominance of roughly 3:1, and is typically unilateral, most often affecting the left kidney.[1,2] The disorder reflects impaired urine flow from the renal pelvis into the proximal ureter, most commonly due to intrinsic narrowing and less frequently from extrinsic compression at the UPJ.[3]

Intrinsic obstruction most commonly results from abnormal smooth muscle development. Other distinct intrinsic causes include disorganized innervation or fibrosis at the UPJ. Regardless of mechanism, intrinsic obstruction leads to impaired peristalsis and urinary drainage. Extrinsic causes are less common and include aberrant crossing vessels, high ureteral insertion, or renal malrotation.[1]

Most children with UPJ obstruction are first identified in utero during routine obstetric US, where antenatal urinary

Figure 1. Fetal US at 35 weeks' gestation demonstrates severe dilation of the right renal pelvis (arrowhead) with associated central and peripheral calyceal dilation (arrow).

Affiliations: Central Michigan University, College of Medicine, Mount Pleasant, Michigan (Chamdi); Phoenix Children's Hospital, Phoenix, Arizona (RB Towbin, Schaefer); Cincinnati Children's Hospital and University of Cincinnati College of Medicine, Cincinnati, Ohio (AJ Towbin).

Disclosures: The authors have no conflicts of interest to disclose. None of the authors received outside funding for the production of this original manuscript and no part of this article has been previously published elsewhere.

https://doi.org/10.37549/JPCR-26-0077

Figure 2. Fetal MRI demonstrates severe right pelvocaliectasis with marked calyceal dilation (arrow). No hydroureter is identified.

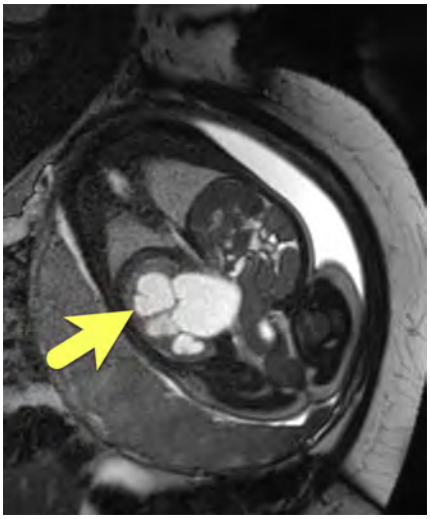

Figure 3. Postnatal renal US performed at 1 month of life demonstrates severe right pelvocaliectasis with dilation of the renal pelvis (arrowhead) and intrarenal calyces (arrow). No hydroureter is present.

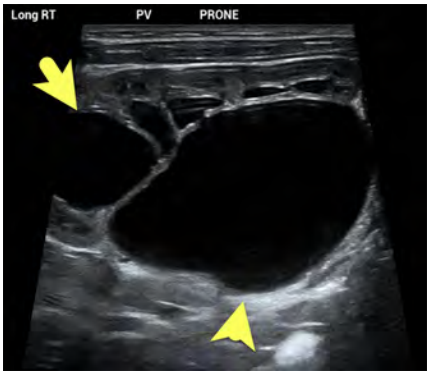

Figure 4. (A) Posterior projection from dynamic images from technetium Tc-99m mercaptoacetyltriglycine diuretic renography demonstrates prompt radiotracer uptake and spontaneous drainage of the left kidney. The right kidney shows delayed parenchymal uptake and excretion. (B) On the renogram curve, the left kidney (dashed line on curve) demonstrates normal washout, whereas the right kidney (solid line on curve) shows delayed parenchymal washout and continued accumulation of tracer within the collecting system, consistent with obstruction. The T½ of the right kidney measured 87 minutes.

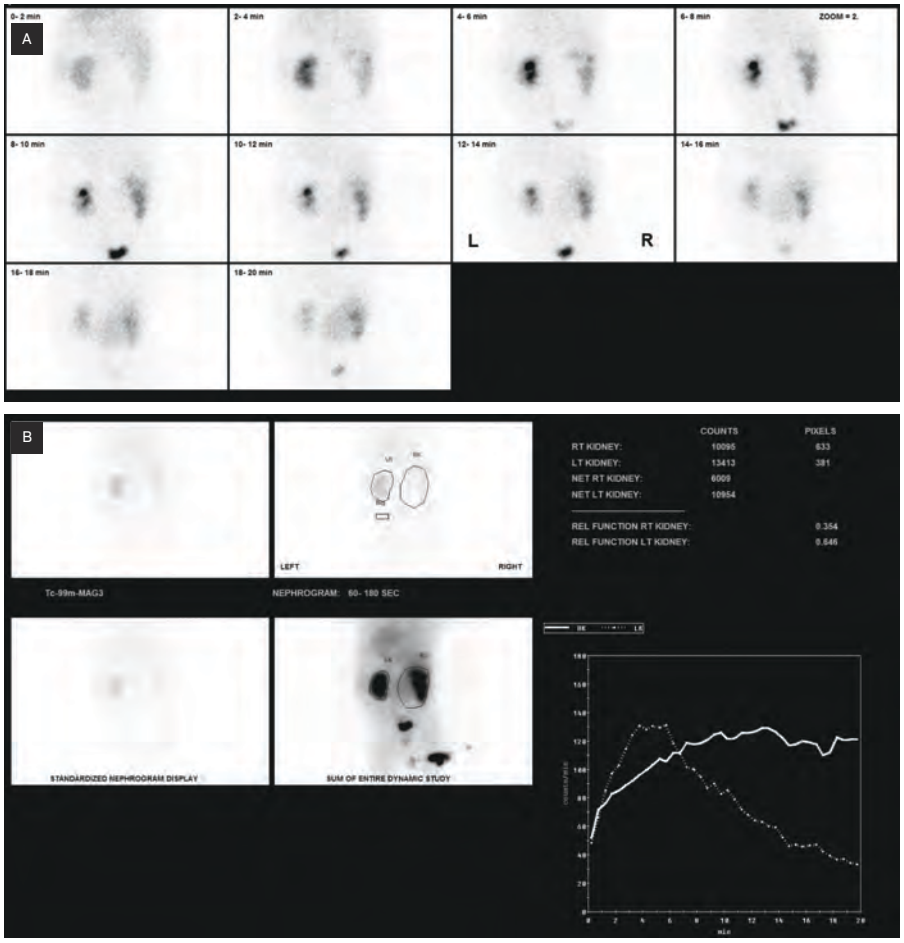

tract dilation is identified.[4] Postnatal evaluation then determines whether the dilation represents physiologic variation or true obstruction. When not diagnosed prenatally, presentation varies. In the neonatal period or later in childhood, patients may develop intermittent, crampy abdominal or flank pain accompanied by nausea and vomiting due to episodic dilation of the collecting system, a presentation referred to as Dietl's crisis.[5]

Postnatal diagnosis relies primarily on US, which demonstrates dilation of the renal pelvis and calyces without ureteral dilation.[6,7] Evaluation should be performed when the infant is well hydrated, with images obtained before and after voiding. The urinary tract dilatation (UTD) classification system provides a standardized framework for describing urinary tract dilation and stratifying its severity but does not establish a specific diagnosis.[8]

Although US is well suited for evaluating the collecting system, it may not identify all causes of obstruction. When additional anatomic detail is required, CT and particularly MR urography allow more comprehensive evaluation, especially when extrinsic causes such as crossing vessels, ureteral kinking, or renal malrotation are suspected. Crossing vessels should be carefully assessed with Doppler US, CT, or MRI to identify a potential source of obstruction and assist in surgical planning.[9] Functional MR urography provides both quantitative functional assessment and high-resolution anatomy without radiation exposure but is generally reserved for complex cases and preoperative planning.[7,10]

Renal function is most assessed with technetium Tc-99m MAG-3 diuretic renography, which evaluates drainage and differential renal function following administration of furosemide. The half-time of tracer clearance is

Figure 5. Intraoperative ureteroscopy images demonstrate cannulation of the right ureter with contrast injection. (A) A jet of contrast (dashed arrow) fills the markedly dilated right renal pelvis. (B) With continued injection, the collecting system opacifies, and markedly dilated calyces (arrow) are visualized.

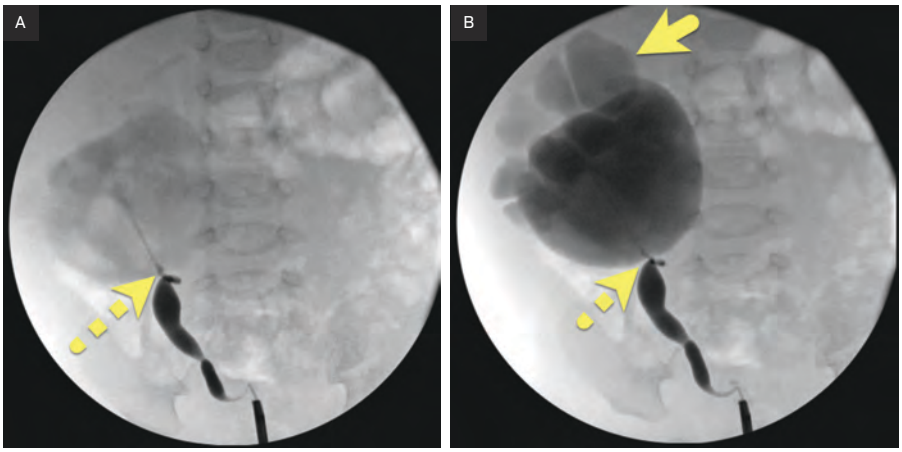

measured, with values greater than 20 minutes typically indicating significant obstruction.[4,10] Although renal scintigraphy provides important functional information, it offers limited anatomic detail.

Management is individualized and depends on renal function, severity of dilation, symptoms, and underlying anatomy. Most children are managed conservatively with serial US and functional assessment, as many cases resolve spontaneously, although approximately 20% ultimately require intervention. Surgical pyeloplasty remains the gold standard and is indicated in patients with high-grade UTD, declining or reduced differential renal function, persistent or worsening symptoms, or recurrent infection.[11] The Anderson-Hynes dismembered pyeloplasty is the most performed technique and may be carried out via open, laparoscopic, or robotic approaches. The procedure involves excision of the narrowed UPJ segment and reanastomosis of the ureter to the renal pelvis.[11]

Recurrent obstruction has been reported in up to 7% of cases and warrants close postoperative follow-up.[12] Long-term sequelae, including early-onset hypertension and proteinuria, should also be monitored, particularly in patients with bilateral disease.[11-13] Despite these potential complications, surgical outcomes are generally favorable, with high long-term success rates.

Conclusion

UPJ obstruction is the most common cause of congenital hydronephrosis and typically presents with dilation of the renal pelvis and calyces without associated ureteral dilation. Although many cases are suspected prenatally as urinary tract dilation, definitive evaluation occurs postnatally through integration of US findings and functional assessment.

US remains the primary imaging modality, with CT or MR urography used when additional anatomic detail is required, particularly to evaluate for extrinsic causes. Renal drainage and differential function are most commonly assessed with MAG-3 diuretic renography. Management is individualized based on symptoms, severity of dilation, and renal function. While many children are managed conservatively, surgical pyeloplasty is indicated in patients with significant obstruction or declining function and is associated with favorable long-term outcomes.

References

1) Williams B, Tareen B, Resnick MI. Pathophysiology and treatment of ureteropelvic junction obstruction. *Curr Urol Rep*. 2007;8(2):111-117. doi: 10.1007/s11934-007-0059-8

2) Fwu C-W, Barthold JS, Mendley SR, et al. Epidemiology of infantile ureteropelvic junction obstruction in the US. *Urology*. 2024;183:185-191. doi:10.1016/j.urology.2023.09.024

3) Tsai J-D, Huang F-Y, Lin C-C, et al. Intermittent hydronephrosis secondary to ureteropelvic junction obstruction: clinical and imaging features. *Pediatrics*. 2006;117(1):139-146. doi:10.1542/peds.2005-0583

4) Cai PY, Lee RS. Ureteropelvic junction obstruction/hydronephrosis. *Urol Clin North Am*. 2023;50(3):361-369. doi:10.1016/j.ucl.2023.04.001

5) Potenta SE, D'Agostino R, Sternberg KM, Tatsumi K, Perusse K. CT urography for evaluation of the ureter. *Radiographics*. 2015;35(3):709-726. doi:10.1148/rg.2015140209

6) Kleiner B, Callen PW, Filly RA. Sonographic analysis of the fetus with ureteropelvic junction obstruction. *AJR Am J Roentgenol*. 1987;148(2):359-363. doi:10.2214/ajr.148.2.359

7) Meshaka R, Biassoni L, Leung G, Mushtaq I, Hiorns MP. Radiological and surgical correlation of pelviureteric junction obstruction in positional anomalies of the kidney in children. *Pediatr Radiol*. 2023;53(3):544-557. doi:10.1007/s00247-022-05557-7

8) Riccabona M, Lobo M-L, Ording-Muller L-S, et al. European society of paediatric radiology abdominal imaging task force recommendations in paediatric uroradiology, part IX: imaging in anorectal and cloacal malformation, imaging in childhood ovarian torsion, and efforts in standardising paediatric uroradiology terminology. *Pediatr Radiol*. 2017;47(10):1369-1380. doi:10.1007/s00247-017-3837-6

9) Nguyen HT, Phelps A, Coley B, et al. 2021 update on the Urinary Tract Dilation (UTD) classification system: clarifications, review of the literature, and practical suggestions. *Pediatr Radiol*. 2022;52(4):740-751. doi:10.1007/s00247-021-05263-w

10) Houat AP, Guimarães CTS, Takahashi MS, et al. Congenital anomalies of the upper urinary tract: a comprehensive review. *Radiographics*. 2021;41(2):462-486. doi:10.1148/rg.2021200078

11) Szavay P, Zundel S. Surgery of uretero-pelvic junction obstruction (UPJO). *Semin Pediatr Surg*. 2021;30(4):151083. doi:10.1016/j.sempedsurg.2021.151083

12) Chen R, Jiang C, Li X, et al. Analysis of risk factors for stenosis after laparoscopic pyeloplasty in the treatment of ureteropelvic junction obstruction. *Int Urol Nephrol*. 2024;56(6):1911-1918. doi:10.1007/s11255-023-03906-5

13) Zouari M, Dghaies R, Rhaiem W, et al. Risk factors for adverse outcomes after pediatric pyeloplasty: a retrospective cohort study. *Int J Urol*. 2024;31(1):45-50. doi:10.1111/iju.15305

Tracheobronchomalacia

Jessica E. Guido, BS; Richard B. Towbin, MD; Carrie M. Schaefer, MD; Alexander J. Towbin, MD

Abstract

Pediatric tracheobronchomalacia is typically classified as primary disease. Patients commonly present with a "barking" or "brassy" cough, wheezing, and stridor. Other signs and symptoms include cyanosis, breathing difficulties, and frequent respiratory tract infections. Dynamic CT or MRI is the preferred imaging modality. On imaging, the airway is shown to collapse during expiration. Patients are supported medically in most instances. However, those with severe symptoms may be treated surgically.

Keywords: airway, chest, congenital

Case Summary

An older child with a history of cystic fibrosis presented for surveillance CT imaging.

Imaging Findings

High-resolution chest CT (Figure 1) with inspiration and expiration shows a smaller caliber of the trachea and bronchi on expiration.

Diagnosis

Tracheobronchomalacia.

The clinical differential diagnosis for tracheobronchomalacia in adolescents includes subglottic stenosis, epiglottitis, vocal cord paralysis, bronchiolitis, subglottic stenosis, and syndromes such as Ehlers-Danlos.

Discussion

Tracheobronchomalacia refers to the dynamic collapse of large airways.[1] The broad nature of the term makes it difficult to make a precise diagnosis. Tracheobronchomalacia can be primary in patients born with a collapsible airway, which may occur because of abnormal division of the esophagus and trachea during foregut separation.[2] Causes include idiopathic, prematurity, or a result of genetic conditions such as Ehlers-Danlos syndrome, Hunter and Hurler syndromes, and trisomy 9 and 21. Secondary tracheomalacia can be from chronic pulmonary inflammation, trauma, masses compressing the airway, and long-term compression that weakens the tracheal cartilage. It is also associated with conditions that cause breakdown of the tracheal cartilage, such as prolonged tracheobronchitis, compression of nearby anatomy, intubation, and relapsing polychondritis, to name a few.[2] Most children with tracheobronchomalacia have primary disease.

Primary tracheobronchomalacia occurs with an incidence between 1 in 1445 and 1 in 2100 live births. Most affected children are male (58-82% of cases). While it is more common in premature infants, tracheobronchomalacia can occur in term infants. Minor airway collapse may improve by 1-2 years of age. However, children with congenital cartilage disorders may experience worsening of symptoms over time.

Children with primary tracheobronchomalacia present with a "barking" or "brassy" cough, breathing difficulties, wheezing, biphasic stridor, cyanosis, and repeated respiratory tract infections.

Although tracheobronchomalacia has traditionally been diagnosed using laryngoscopy and bronchoscopy, noninvasive airway imaging has become increasingly popular.[3] Inspiratory-expiratory airway fluoroscopy has been used with increasing frequency. However, recent studies have shown it to have low sensitivity and specificity, making it a less useful tool.[4] Dynamic MRI and CT have also been used to diagnose tracheobronchomalacia. One study found that dynamic CT is highly accurate, performing similarly to laryngoscopy and bronchoscopy in diagnosis and visualization of tracheobronchomalacia.[5] The non-invasive nature of the CT makes it a valuable diagnostic tool and first diagnostic choice in many instances. At maximal inspiration, the trachea should appear round or oval and the lungs expanded. Normally, at maximal expiration, the aeration of the lungs decreases. However, the

Affiliations: University of Arizona College of Medicine-Phoenix Campus, Phoenix, Arizona (Guido); Department of Radiology, Phoenix Children's Hospital, Phoenix, Arizona (RB Towbin, Schaefer); Department of Radiology, Cincinnati Children's Hospital, University of Cincinnati College of Medicine, Cincinnati, Ohio (AJ Towbin).

Disclosures: The authors have no conflicts of interest to disclose. None of the authors received outside funding for the production of this original manuscript and no part of this article has been previously published elsewhere.

https://doi.org/10.37549/JPCR-26-0076

Figure 1. (A, B) Axial chest CT images at the level of the thoracic inlet, (C, D) carina, and (E, F) bronchus intermedius during inspiration and expiration respectively show a narrowed caliber of the trachea and bronchi on expiration. (G, H) Coronal minimum intensity projection images during inspiration and expiration show a smaller caliber of more peripheral airways on expiration.

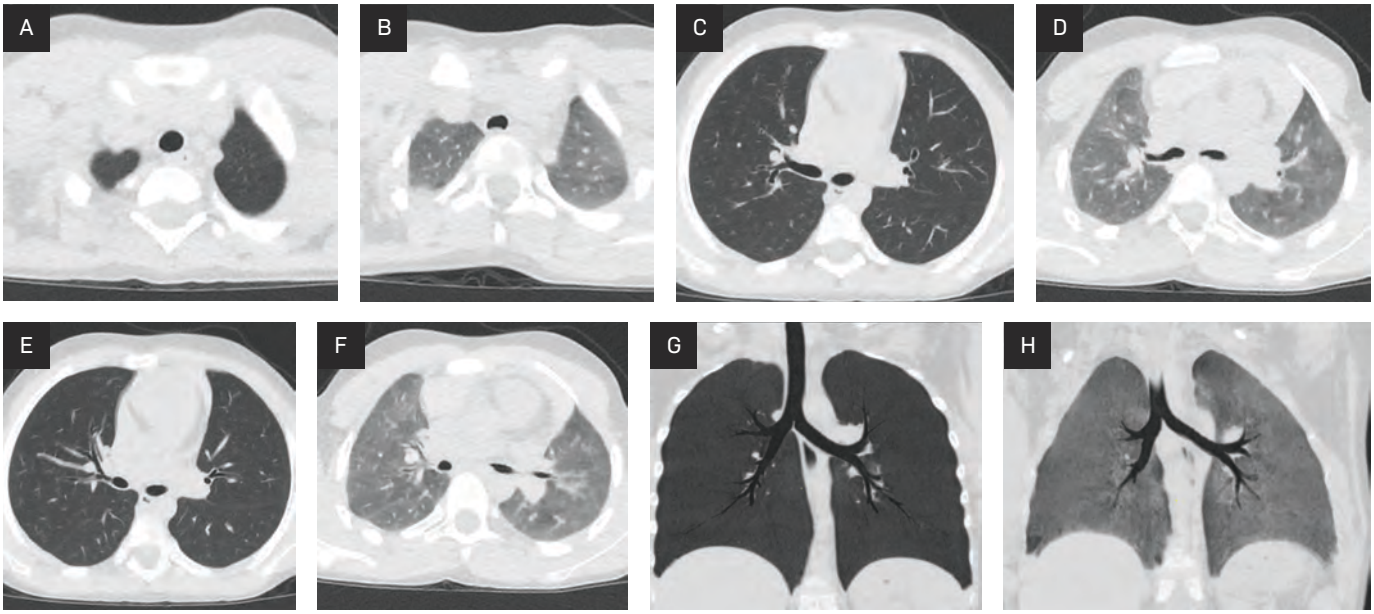

appearance of the trachea is unchanged. In patients with tracheobronchomalacia, the trachea collapses with flattening or forward bowing of the posterior tracheal wall, causing 50% or more expiratory reduction in the cross-sectional area of the trachea or bronchi, which is diagnostic.[6] When tracheobronchomalacia is comorbid with cartilaginous disorders, concentric narrowing may also be seen.

Tracheobronchomalacia is managed medically or, in severe cases, with surgery. Currently, there is no standard therapy. Medical management can include medications to decrease mucous secretions, low-dose inhaled corticosteroids to decrease inflammation, and control of gastroesophageal reflux. Surgical intervention is available for children with severe disease who do not improve with medical management. Common surgical interventions include silicone or mesh stent placement, tracheostomy, anterior/posterior tracheopexy, or tracheobronchial resection and reconstruction.[7,8]

Conclusion

Pediatric tracheobronchomalacia is typically classified as primary disease. Patients most commonly present with a "barking" or "brassy" cough, wheezing, and stridor. Other signs and symptoms include cyanosis, breathing difficulties, and frequent respiratory tract infections. Dynamic CT or MRI is the preferred imaging modality. On imaging, the airway is shown to collapse during expiration. Patients are supported medically in most instances. However, those with severe symptoms may be treated surgically.

References

1) Yang D, Cascella M. Tracheomalacia; 2021. https://www.ncbi.nlm.nih.gov/books/NBK553191

2) Choi S, Lawlor C, Rahbar R, et al. Diagnosis, classification, and management of pediatric tracheobronchomalacia: a review. *JAMA Otolaryngol Head Neck Surg*. 2019;145(3):265-275. doi:10.1001/jamaoto.2018.3276

3) McLaren CA, Roebuck DJ. Imaging tracheobronchomalacia in the 21st century. *J Med Imaging Radiat Oncol*. 2012;56(2):129-131. doi:10.1111/j.1754-9485.2012.02357.x

4) Emmett S, Megow A, Woods C, Wood J. Poor correlation between airway fluoroscopy and rigid bronchoscopic evaluation in paediatric tracheomalacia. *Int J Pediatr Otorhinolaryngol*. 2022;158:111157. doi:10.1016/j.ijporl.2022.111157

5) Ngerncham M, Lee EY, Zurakowski D, Tracy DA, Jennings R. Tracheobronchomalacia in pediatric patients with esophageal atresia: comparison of diagnostic laryngoscopy/bronchoscopy and dynamic airway multidetector computed tomography. *J Pediatr Surg*. 2015;50(3):402-407. doi:10.1016/j.jpedsurg.2014.08.021

6) Lee EY, Boiselle PM. Tracheobronchomalacia in infants and children: multidetector CT evaluation. *Radiology*. 2009;252(1):7-22. doi:10.1148/radiol.2513081280

7) Kamran A, Zendejas B, Jennings RW. Current concepts in tracheobronchomalacia: diagnosis and treatment. *Semin Pediatr Surg*. 2021;30(3):151062. doi:10.1016/sempedsurg.2021.151062

8) Shieh HF, Smithers CJ, Hamilton TE, et al. Posterior tracheopexy for severe tracheomalacia. *J Pediatr Surg*. 2017;52(6):951-955. doi:10.1016/j.pedsurg.2017.03.018